Available online at www.sciencedirect.com
ScienceDirect
Nuclear Instruments and Methods in Physics Research B 266 (2008) 4403–4406
NIM B
Beam Interactions with Materials & Atoms
www.elsevier.com/locate/nimb

Resonant laser ionization of polonium at RILIS-ISOLDE for the study of ground- and isomer-state properties

Thomas E. Cocolios [a], Bruce A. Marsh [b,*], Valentine N. Fedosseev [b], Serge Franchoo [c], Gerhard Huber [d], Mark Huyse [a], Alexandra M. Ionan [e], Karl Johnston [b], Ulli Köster [f], Yuri Kudryavtsev [a], Maxim Seliverstov [d,e], Etam Noah [b], Thierry Stora [b], Piet Van Duppen [a]

[a] *Instituut voor Kern- en Stralingsfysica, Katholieke Universiteit Leuven, B-3001 Leuven, Belgium*
[b] *ISOLDE, CERN, CH-1211 Geneva 23, Switzerland*
[c] *Institut de Physique Nucléaire, F-91406 Orsay cedex, France*
[d] *Institut für Physik, Johannes Gutenberg Universität, D-55099 Mainz, Germany*
[e] *Petersburg Nuclear Physics Institute, 188350 Gatchina, Russia*
[f] *Institut Laue Langevin, F-38042 Grenoble cedex 9, France*

Available online 19 June 2008

Abstract

Three new ionization schemes for polonium have been tested with the resonant ionization laser ion source (RILIS) during the on-line production of ^{196}Po in a UC_x target at ISOLDE. The saturation of the atomic transitions has been observed and the yields of the isotope chain $^{193–198,200,202,204}$Po have been measured. This development provides the necessary groundwork for performing in-source resonant ionization spectroscopy on the neutron-deficient polonium isotopes ($Z = 84$).

PACS: 23.60.+e; 27.80.+w; 29.25.Ni; 32.80.Rm; 42.62.Fi

Keywords: Laser ionization; Polonium; Production yield; Optical transition; Saturation

1. Introduction

Shape coexistence effects across the $Z = 82$ proton shell closure is an area of research of high interest to modern nuclear physics. The initial discovery of large isotope shifts and isomeric shifts in the neutron-deficient mercury isotopes ($Z = 80$) [1] from the measurement of the mean-square charge radii illustrated the complexity of the nuclear structure between the $N = 82$ and $N = 126$ neutron shell closures and the importance of excitations through the $Z = 82$ proton shell closure. The nuclear spectroscopic studies of the other elements in the same region of the nuclear chart, namely lead ($Z = 82$) [2] and polonium ($Z = 84$) [3], hinted at the importance of shape coexistence around the neutron mid-shell at $N = 104$.

In recent work at CERN-ISOLDE, the shape of the neutron-deficient lead isotopes was directly observed from the changes in the mean-square charge radius, measured via in-source resonant ionization laser spectroscopy [4]. This study was made possible after the development of a laser excitation scheme for lead at the ISOLDE-RILIS (resonant ionization laser ion source).

In order to perform such a study on the polonium isotopes, an ionization scheme with an excitation step that can be used to determine the changes in the mean-square charge radii is needed. This excitation step will be obtained with a narrow bandwidth scanning laser to probe the resonance profile, yielding the hyperfine structure of the odd-A isotopes and the isotope shift between any two isotopes. As the element polonium does not have a stable isotope, a

* Corresponding author.
E-mail address: bruce.marsh@cern.ch (B.A. Marsh).

0168-583X/$ - see front matter © 2008 Elsevier B.V. All rights reserved.
doi:10.1016/j.nimb.2008.05.142

search for an efficient and effective ionization scheme, in terms of sensitivity to the changes in the mean-square charge radius, has been performed at the ISOLDE on-line separator using radioactive polonium isotopes. This paper reports on the observation of such ionization schemes and their properties.

2. Beam production

The isotopes are produced on-line with the 1.4 GeV CERN-PS booster proton beam impinging on a UC_x target (50 g cm^{-2} of depleted uranium with 99.6% of ^{238}U) at the ISOLDE facility. The produced isotopes diffuse from the high temperature (≈2000 °C) target and enter the RILIS hot cavity where they are resonantly ionized with a three-step laser ionization scheme [5,6]. After extraction and acceleration to 60 keV the ions are separated according to their mass-over-charge ratio with an analysing magnet. Details of the RILIS laser setup can be found in [7] and references therein.

Two different yield measurement setups were used. For measuring the α-emitting $^{193–198}$Po isotopes, the ion beam is implanted into thin carbon foils (30 μg cm^{-2}) mounted on a rotating wheel with 10 foil holders (only 4 were used for this test). The α particles emitted by the decay of the isotopes are detected with a silicon detector (active area 150 mm^2, thickness 300 μm) placed behind the foil position. For the ^{200,202,204}Po isotopes, the ion beam is implanted into a mylar tape at the ISOLDE tape station. The tape is then moved and the β decay is observed along with its associated γ radiation. The yield, expressed in ions μC^{-1}, extracted from each α or γ spectrum, is used to determine the performance of the laser excitation and ionization schemes.

3. Study of the atomic transitions

This study was limited to the study of the three ionization schemes shown in Fig. 1. In the first scheme (shown on the left-hand side of Fig. 1) one valence electron is excited from its ground state with a UV transition at 255.8 nm[1] to a first excited state. The second excited state is reached with an infrared transition at 843.38 nm. An electron occupying this level is sufficiently energetic for subsequent excitation to the continuum by the non-resonant absorption of a 510.6 nm photon, provided by the Cu vapour laser. The UV laser light is produced by tripling the frequency of a beam from a dye laser; its power reaches nearly 100 mW. The infrared laser light is produced with a dye laser and has up to 2 W of available power. The power from the Cu vapour laser used for the final step is 18 W.

The two remaining schemes (shown on the right-hand side of Fig. 1) also use a UV transition to reach the first

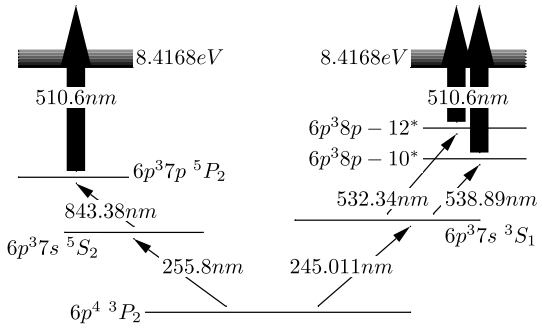

Fig. 1. Laser ionization schemes, from the ground state to over the ionization potential. The last step (510.6 nm) is non-resonant. The exact atomic configuration of the levels marked by a star (∗) is undetermined.

excited state (245.011 nm). From this level both a 532.34 nm and a 538.89 nm transition were investigated and the 510.6 nm Cu vapour laser was used for the non-resonant final step. The laser powers available for each transition were similar to values quoted for the first scheme. All five resonant transitions involve one of the valence electrons in the 7s shell where the interaction with the nucleus is at its highest thus providing the information of interest to nuclear structure such as the change in the mean-square charge radius and the moments of the nucleus.

Ionization of ^{196}Po was achieved with each of the three schemes. Resonance laser ionization was confirmed by the ability to completely suppress the ion production by blocking or de-tuning the UV laser beam. In the case of the UV + infrared ionization scheme, the resonance curve of the second step has been observed confirming the existence of the second excited state. This is the first confirmation of the existence of the excited states that were suggested in [8]. With the direct observation of the succession of the electron excitations, the position of the $6p^3 7p\ ^5P_2$ and the $6p^3 8p$ energy levels is now fixed.

Once each laser beam is optimised in frequency and position to maximise the production, the saturation of each resonant transition is studied. The power of the laser is controlled using an attenuator in the path of the laser beam of interest. Fig. 2 shows the saturation curves of the UV + infrared scheme while Fig. 3 shows the saturation curves of the UV + green schemes. All display the characteristic behaviour of saturated transitions except the UV transition at 255.8 nm; the latter is not saturated, meaning a higher power would further improve the ionization efficiency.

4. Yields of neutron-deficient polonium

The production yields of polonium for $A = 193–198$ and for $A = 200$, 202, 204 are measured from different targets, however in both cases the same target material and ionization scheme (UV + infrared) was used; the yields may therefore vary from one set to the other. The resolution of the α detector is sufficiently high for resolving the ground state from the isomer decay in the case of the odd-A isotopes ^{193,195,197}Po. The acquisition times and

[1] This transition was used by Kowlewska et al. to study the mean-square charge radii of $^{200,202,204–210}$Po and moments of ^{205,207,209}Po [9].

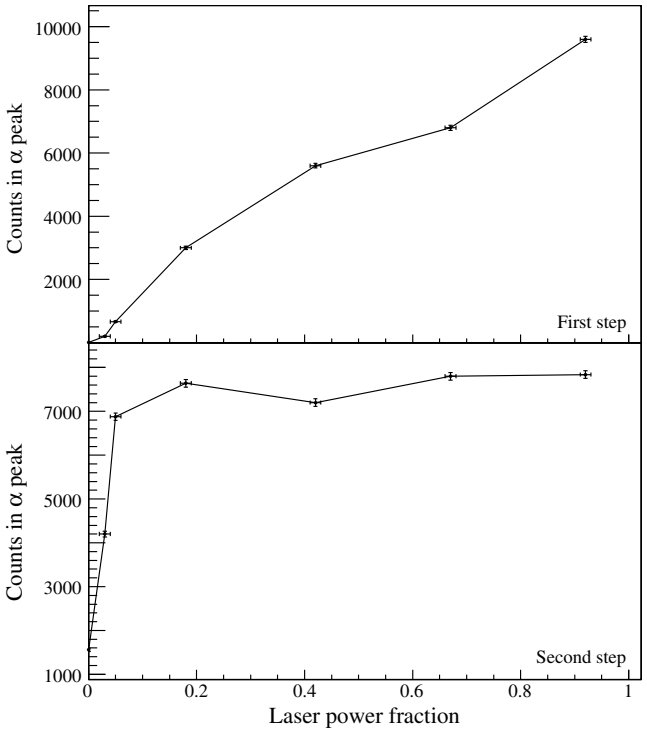

Fig. 2. Saturation curves of the UV + infrared scheme using ^{196}Po. The top figure represents the curve of the first excitation step (255.8 nm) while the bottom figure, that of the second step (843.38 nm). While one transition is studied, the other transitions are kept at their maximal power. The lower figure shows over-saturation, meaning that more power than necessary is available.

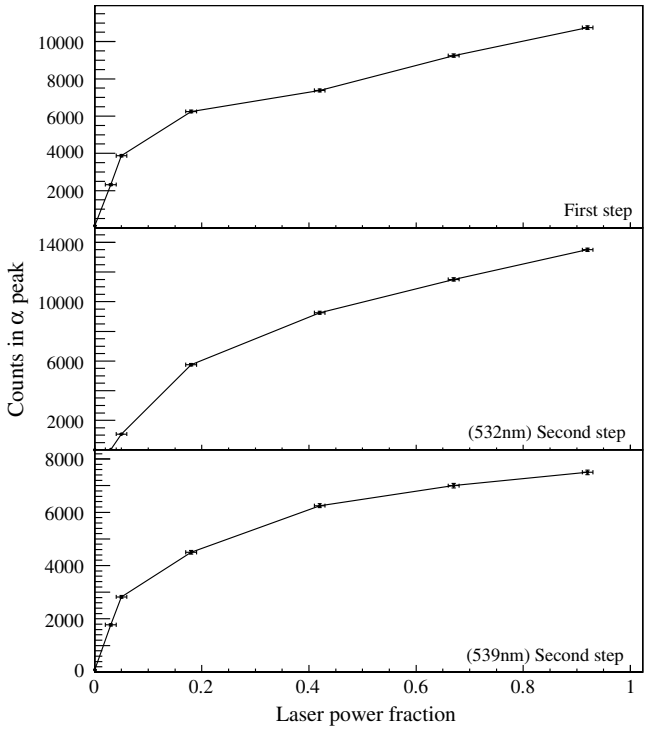

Fig. 3. Saturation curves of the UV + green schemes using ^{196}Po. The top figure represents the curve of the first excitation step (245.011 nm), the middle figure, that of the first possible second step transition (532.34 nm) and the last figure, that of the other possible second step (538.89 nm). While one transition is studied, the other transitions are kept at their maximal power.

the number of protons impinging the target were different for each isotope. The resulting yields, normalised to the proton current in ions μC^{-1}, are shown in Table 1 and displayed in Fig. 4.

The yield curve closely follows the yields obtained previously at the ISOLDE-SC (600 MeV protons) [10] with the unselective MK5 hot plasma ion source [11]. Note that the thickness of ^{238}U target for the latter was only 9.7 g cm^{-2} rather than 50 g cm^{-2} for this work. The advantage of the laser ionization source resides in its selectivity and although some ionization efficiency is lost, most of the contaminants are suppressed by this method. In the course of this work, only the decay of a few ^{193}Bi nuclei was observed as seen in Fig. 5. The contamination of the beam was not the subject of a thorough analysis during this study. A more complete assessment would require consideration of possible β-emitters which are not observed with the α-detection setup. The thallium isotopes, with a low ionization potential, are likely to be efficiently surface ionized. The yield of ^{196}Po has also been measured for the UV + green schemes and was found to be similar to that for the other scheme (Fig. 4).

For stable isotopes, the RILIS ionization efficiency is measured by complete evaporation of a sample with a known amount of atoms into the ion source and integrating the observed ion current after mass separation. Due to the absence of stable polonium isotopes, the overall release and ionization efficiency was instead estimated from a comparison of the measured radio-isotope yields to the in-target production rates based on ^{238}U spallation cross-sections calculated with the ABRABLA code for an incoming 1.4 GeV proton beam. Secondary reactions and feeding from α or EC/β decay precursors are then neglected [12,13]. Fig. 6 shows the trend of the overall efficiency as a function of the polonium isotope half-life. Using ^{202}Po, whose half-life is long enough to be completely released, one can determine a set of parameters to reproduce the release curve measured for ^{202}Po using a triple exponential

Table 1
Polonium yields from the UV + infrared scheme

Isotope	Half-life	Yield (ions μC)	Isomer	Half-life (s)	Yield (ions μC)
^{193g}Po	0.45 s	7.0×10^1	^{193m}Po	0.24	1.0×10^2
^{194}Po	0.39 s	2.7×10^3		–	–
^{195g}Po	4.6 s	2.5×10^4	^{195m}Po	1.9	5.5×10^4
^{196}Po	5.8 s	4.8×10^5		–	–
^{197g}Po	54 s	5.8×10^5	^{197m}Po	26	2.0×10^6
^{198}Po	1.77 m	1.2×10^7		–	–
^{200}Po	11.5 m	6.4×10^6		–	–
^{202}Po	44.6 m	1.7×10^7		–	–
^{204}Po	3.53 h	1.1×10^7		–	–

The yields for each mass are measured with different proton intensities and collection times but normalised to the same unit of ions μC^{-1}. The top and bottom sections of the table correspond to two different targets.

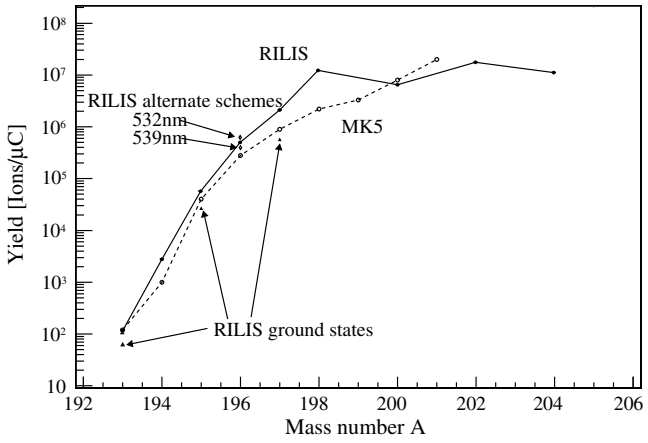

Fig. 4. Yields of $^{193–198,200,202,204}$Po from laser ionization with the UV + infrared scheme (solid line) compared to those from the hot plasma source MK5 (dashed line). Note that the quantity of U in the target was a factor of 5 less in the study of the hot plasma source. The curve for the RILIS goes through the odd isomers while the odd ground states are displayed under the curve. The yields from the UV + green schemes are also measured for ^{196}Po and the two results are shown on the figure, labelled as wavelength of the second step.

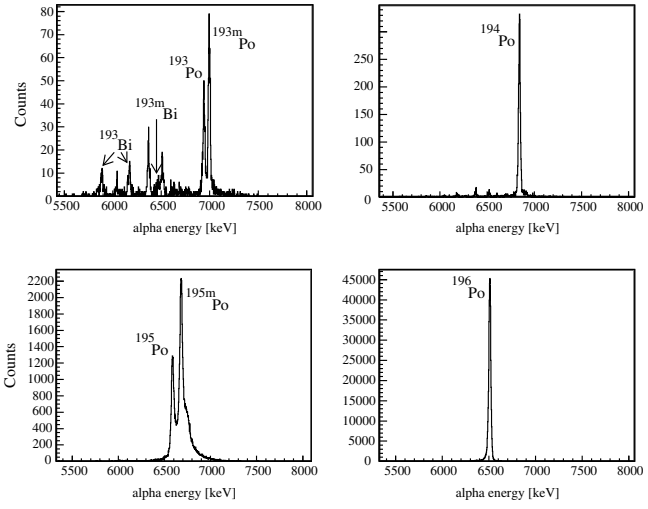

Fig. 5. Alpha spectrum of ^{193,194,195,196}Po. All are acquired with the UV + infrared scheme over 120 s.

approach. Integrating this release curve with the nuclear decay gives the released fraction of polonium for each isotope [14]. This function is then multiplied with the laser ionization efficiency which can now be fitted to the data, yielding a final result of 0.4%. This value is only a lower limit as the ABRABLA calculations in this region are known to over-estimate the production and a proportion of the polonium could be irreversibly trapped in the target.

5. Conclusion

Three different laser ionization schemes of polonium have been successfully tested on-line at the ISOLDE-RILIS. All schemes perform well and yields suitable for in-source laser spectroscopy measurements are achievable. The overall efficiency is limited by the very slow release of polonium. A lower limit for the laser ionization efficiency of 0.4% has been determined. This opens new possibilities for the study of neutron-deficient polonium isotopes where shape staggering effects are expected [3]. The first study will be on the change in mean-square charge radius of the neutron-deficient polonium isotopes by in-source laser spectroscopy as used for studying lead and bismuth isotopes [4,15].

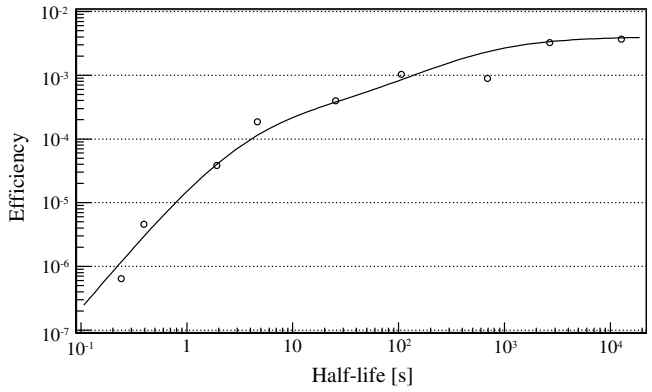

Fig. 6. The circles represent the product of the release and the ionization efficiency of polonium isotopes, deduced from a comparison of the measured yields with calculations using the ABRABLA code for 1.4 GeV protons with no secondary reaction [12,13], while the solid line represents the fit to those values of a convolution of the release to the isotope half-life. The isotope and half-life ordering from ^{193}Po to ^{204}Po is similar. In the case of the odd isotopes, only the isomer is considered.

Acknowledgements

The authors would like to acknowledge the contribution of Martin Eller. This work was performed thanks to the support of the European Union Sixth Framework through RII3-EURONS (Contract No. 506065), the BRIX-IAP Research Program No. P06/23 and FWO Vlaanderen (Belgium).

References

[1] G. Ulm et al., Z. Phys. A 325 (1986) 247.
[2] A.N. Andreyev et al., Nature 405 (2000) 430.
[3] A.N. Andreyev et al., Phys. Rev. Lett. 82 (1999) 1819.
[4] H. De Witte et al., Phys. Rev. Lett. 98 (2007) 112502.
[5] E. Kugler, D. Fiander, B. Jonson, H. Haas, A. Przewloka, H.L. Ravn, D.J. Simon, K. Zimmer, and the ISOLDE Collaboration, Nucl. Instr. and Meth. B 70 (1992) 41.
[6] U. Köster et al., Nucl. Instr. and Meth. B 204 (2003) 347.
[7] V.N. Feddosseev, in: Proceedings of the EMIS2007 Conference, Nucl. Instr. and Meth. B (2007).
[8] G.W. Charles, J. Opt. Soc. Am. 56 (1966) 1292.
[9] D. Kowalewska, K. Bekk, S. Göring, A. Hanser, W. Kälber, G. Meisel, H. Rebel, Phys. Rev. A 44 (1991) R1442.
[10] E. Hagebø, P. Hoff, O.C. Jonsson, E. Kugler, J.P. Omtvedt, H.L. Ravn, K. Steffensen, Nucl. Instr. and Meth. B 70 (1992) 165.
[11] S. Sundell, H. Ravn, Nucl. Instr. and Meth. B 70 (1992) 160.
[12] S. Lukić, private communication, 2007.
[13] S. Lukić, F. Gevaert, A. Kelić, M.V. Ricciardi, K.-H. Schmidt, O. Yordanov, Nucl. Instr. and Meth. A 565 (2006) 784.
[14] M. Eller, S. Miksch, J. Lettry, T. Stora, R. Catherall, Eur. Phys. J. – Special Topics 150 (2007) 233.
[15] B.M. Marsh, M. Seliverstov, et al., in: Proceedings of the EMIS2007 Conference, Nucl. Instr. and Meth. B (2007).